ADVANCES IN ATMOSPHERIC SCIENCES, VOL. 35, NOVEMBER 2018, 1372–1380

• **Original Paper** •

Predictable and Unpredictable Components of the Summer East Asia–Pacific Teleconnection Pattern

Xiaozhen LIN[1,2], Chaofan LI[*3], Riyu LU[1,2], and Adam A. SCAIFE[4,5]

[1]*State Key Laboratory of Numerical Modelling for Atmospheric Sciences and Geophysical Fluid Dynamics, Institute of Atmospheric Physics, Chinese Academy of Sciences, Beijing* 100029*, China*

[2]*University of Chinese Academy of Sciences, Beijing* 100029*, China*

[3]*Center for Monsoon System Research, Institute of Atmospheric Physics, Chinese Academy of Sciences, Beijing* 100029*, China*

[4]*Met Office Hadley Centre, FitzRoy Road, Exeter* EX1 3PB*, UK*

[5]*College of Engineering, Mathematics and Physical Sciences, University of Exeter, Exeter, Devon* EX4 4QF *UK*

(Received 17 December 2017; revised 21 April 2018; accepted 06 June 2018)

ABSTRACT

The East Asia–Pacific (EAP) teleconnection pattern is the dominant mode of circulation variability during boreal summer over the western North Pacific and East Asia, extending from the tropics to high latitudes. However, much of this pattern is absent in multi-model ensemble mean forecasts, characterized by very weak circulation anomalies in the mid and high latitudes. This study focuses on the absence of the EAP pattern in the extratropics, using state-of-the-art coupled seasonal forecast systems. The results indicate that the extratropical circulation is much less predictable, and lies in the large spread among different ensemble members, implying a large contribution from atmospheric internal variability. However, the tropical–mid-latitude teleconnections are also relatively weaker in models than observations, which also contributes to the failure of prediction of the extratropical circulation. Further results indicate that the extratropical EAP pattern varies closely with the anomalous surface temperatures in eastern Russia, which also show low predictability. This unpredictable circulation–surface temperature connection associated with the EAP pattern can also modulate the East Asian rainband.

Key words: EAP pattern, circulation, seasonal forecast, surface temperature, eastern Russia

Citation: Lin, X. Z., C. F. Li, R. Y. Lu, and A. A. Scaife, 2018: Predictable and unpredictable components of the summer East Asia–Pacific teleconnection pattern. *Adv. Atmos. Sci.*, **35**(11), 1372–1380, https://doi.org/10.1007/s00376-018-7305-5.

1. Introduction

The East Asia–Pacific (EAP) teleconnection pattern (Huang and Sun, 1992), which is also referred to as the Pacific–Japan pattern (Nitta, 1987), dominates the interannual variability of summer climate over the western North Pacific and East Asia (WNP-EA). It features anomalous zonally elongated centers that appear alternately between the equator and high latitudes in the meridional direction over the WNP-EA (Kosaka and Nakamura, 2006; Lu and Lin, 2009). The circulation anomalies associated with the EAP pattern exhibit a meridional wave-like distribution with alternate cyclonic and anticyclonic anomalies (e.g., Kosaka and Nakamura, 2006, Fig. 4; Lu and Lin, 2009, Fig. 2). The EAP pattern links closely with variation of the circulation not only over the subtropical WNP, manifesting as a change in the WNP subtropical high (Lu and Dong, 2001; Lu, 2004), but also over the midlatitude WNP-EA. This teleconnection pattern modifies water vapor transport and significantly influences summer rainfall over East Asia.

Anomalous convection around the Philippine Sea is generally recognized as one of the wave sources for the EAP pattern, which propagates northward in the lower troposphere (Kawamura et al., 1996; Lu, 2001; Kosaka and Nakamura, 2006). Nevertheless, the wave activity excited by the anomalous convection around the Philippine Sea appears mainly in the low-latitude regions to the south of 35°N (Kosaka and Nakamura, 2006). In view of the remarkable circulation anomalies over midlatitude regions of the WNP-EA associated with the EAP teleconnection pattern, it suggests that the underlying physical mechanisms may be related to Rossby wave propagation into the midlatitude regions (e.g., Scaife et al., 2017), but the mechanisms behind the EAP pattern are not fully understood.

As for the prediction of the EAP teleconnection pattern, forecast models generally capture the component associated with the tropical air–sea interactions (Kosaka et al., 2012, 2013; Li et al., 2012, 2014a). These good forecasts manifest mainly over the subtropical WNP as variation of the

* Corresponding author: Chaofan LI
Email: lichaofan@mail.iap.ac.cn

WNP subtropical high (Wang et al., 2009; Li et al., 2012). In the lower troposphere, high prediction skill shown by current coupled forecast systems is found over the WNP south of Japan for the zonal wind (Li et al., 2012). However, the prediction skill decreases rapidly northward to the midlatitude regions, particularly north of 35°N. In particular, the lower-tropospheric circulation related to the WNP subtropical high shows significant correlation with an anomalous cyclone or anticyclone over the midlatitude regions in observations, but no notable anomalies in the ensemble mean model output, as illustrated in Li et al. (2012). This implies either that this high-latitude component is simply unpredictable or that current coupled models may not capture the observed midlatitude components of the EAP pattern. It further suggests that different (unpredictable) mechanisms are responsible for the midlatitude circulation associated with the EAP pattern, in addition to the tropical forcing. It is crucial to gain a better understanding of the underlying mechanism for the variation of the midlatitude circulation associated with the EAP teleconnection pattern, since this midlatitude circulation significantly affects the summer climate over East Asia.

The summer of 1998 is special for several aspects. First, the EAP teleconnection pattern is clear in this summer (Fig. 1a). Second, associated with this EAP pattern, there is a strong anticyclonic anomaly over the WNP, which is typical for the El Niño decaying summer and leads to floods in East Asia (e.g., Wang et al., 2000; Xie et al., 2016; Li et al., 2017). Finally, and most importantly, associated with strong tropical signals, the climate anomalies of this summer, at least in the tropics and subtropics, show high prediction skill (Li et al., 2012; MacLachlan et al., 2015). Therefore, this summer provides a good opportunity for us to investigate tropical–extratropical interaction. For this purpose, in this study we analyze the outputs of state-of-the-art coupled seasonal forecast systems, and compare the model results with observations.

The organization of this paper is as follows: Section 2 introduces the data used. Section 3 analyzes the prediction of the EAP teleconnection pattern in 1998 and the related responses of summer prediction for surface temperature and precipitation. Section 4 provides a summary and discussion.

2. Observed datasets and retrospective forecasts

We use the monthly mean National Centers for Environmental Prediction–National Centers for Atmospheric Research reanalysis data (Kalnay et al., 1996) from 1979 to 2015 in summer (June–July–August). We also use precipitation data from the Global Precipitation Climatology Project dataset (Adler et al., 2003), from 1979 to 2015. Here, we only focus on the interannual variation and exclude the decadal or long-term component by removing a nine-year running average.

Two sets of retrospective forecast (hindcast) data are examined in this study. The first is from the Ensembles-Based Predictions of Climate Change and their Impacts (ENSEMBLES) seasonal forecast project (Van Der Linden and Mitchell, 2009), which was an EU-funded integrated prediction project based on five coupled atmosphere–ocean–land global models. It comprises hindcasts for the 46-year period of 1960–2005. For each year, seasonal forecasts were initialized on 1 May and run for seven months with nine members for each model. Therefore, there are 45 members for each year.

We also use output from the Met Office Global Seasonal forecast system 5 (GloSea5) (MacLachlan et al., 2015). Hindcasts from GloSea5 increase the ensemble size in our study; plus, GloSea5 exhibits good prediction skill for East Asian precipitation and the WNP subtropical high (MacLachlan et al., 2015; Li et al., 2016). The model used in this forecast system is the Hadley Center Global Environmental Model version 3, with a horizontal resolution of $0.83° \times 0.56°$ for the atmosphere and 0.25° for the ocean and sea-ice model. The retrospective forecasts in GloSea5 were performed for each summer from 1992 to 2011, with 24 members each year.

The two hindcasts show similarity in the simulation of the EAP teleconnection pattern. The temporal correlation coefficient for the EAP index [defined by Huang (2004)] between the ENSEMBLES (GloSea5) system and observations during 1960–2005 (1992–2011) is 0.57 (0.50). Therefore, we combine all the ensemble members for 1998 in these two forecast systems together to investigate the predictability, with sufficient ensemble members (69) and using the overlapping hindcast period (1992–2005) as climatology, and the anomalies are calculated by removing the climatology of the ensemble mean.

3. Results

3.1. *Prediction of the EAP teleconnection pattern in 1998*

Figure 1 shows the 850-hPa horizontal wind anomalies in observations and model predictions in 1998. In observations, the wind anomalies over the WNP-EA present a clear meridional teleconnection pattern with three centers along East Asia (Fig. 1a). There are two anomalous anticyclones over the Philippine Sea and Northeast Asia, and one anomalous cyclone over East Asia. The multi-model ensemble (MME) mean result, by contrast, shows horizontal wind anomalies in the midlatitude regions that are small compared with the anticyclonic anomalies over the subtropical WNP (Fig. 1b). The MME mean result only predicts the anticyclonic anomalies over the subtropical WNP. The extratropical part of the EAP teleconnection pattern is not well predicted in the ensemble mean, despite the strong tropical forcing in the year of 1998. There are two possible causes of this difference: the extratropical EAP nodes could simply be unpredictable, or there could be model errors preventing its simulation in response to tropical forcing. To assess this further we examine the model integration members to determine if they can simulate the extratropical part of the EAP pattern via internal unpredictable variability in the model.

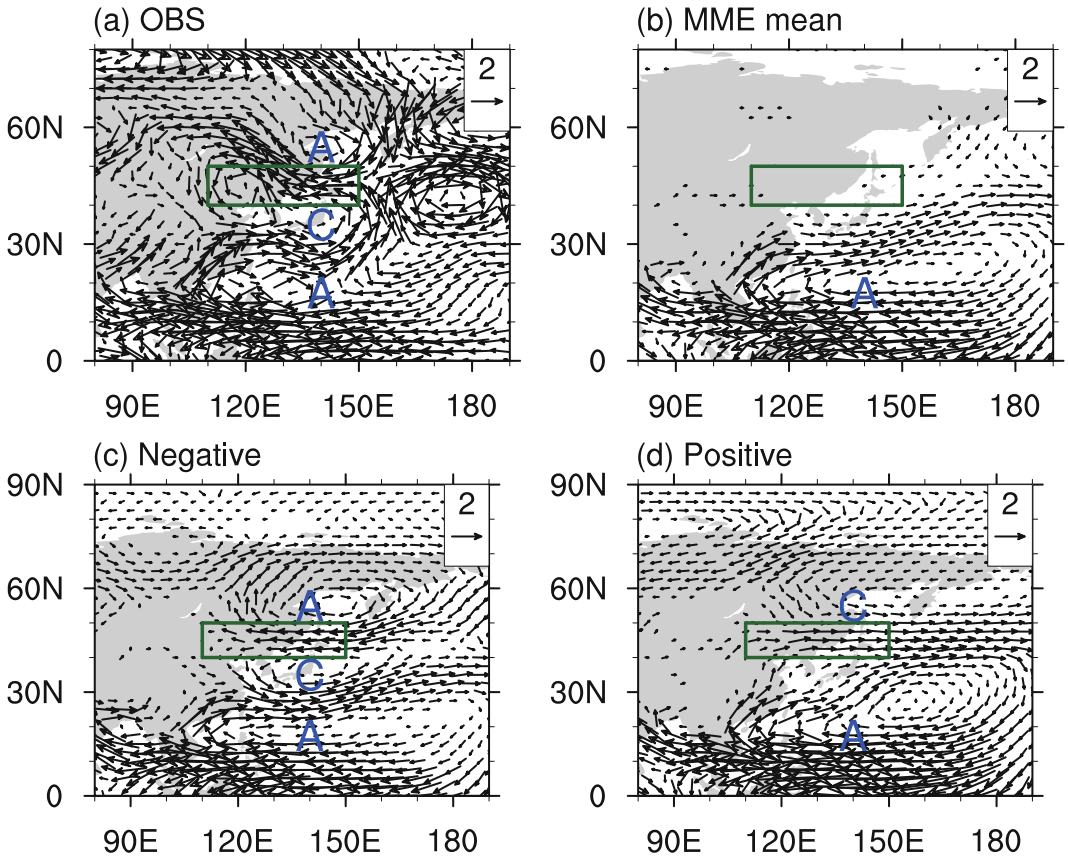

Fig. 1. 850-hPa horizontal wind anomalies in the (a) observation and (b) MME mean in 1998. Composite 850-hPa horizontal wind anomalies for (c) negative integration members and (d) positive integration members in 1998 (units: m s^{-1}). The "A" and "C" represent anticyclonic and cyclonic circulation anomalies, respectively. The green box indicates the domain of the midlatitude component of the EAP teleconnection pattern (40°–50°N, 90°–150°E).

According to the distinct difference of 850-hPa horizontal wind anomalies between observations and the MME mean prediction, the zonal wind anomalies over (40°–50°N, 110°–150°E) is defined as the midlatitude zonal wind index. To avoid the influence of the anticyclonic anomalies over the subtropical WNP, only the north part of cyclonic anomalies is adopted to define the index, for further investigation of the teleconnection between midlatitude zonal wind and the tropical part of the EAP pattern. A positive (negative) zonal wind index represents westerly (easterly) wind anomalies in the midlatitudes. In total, 11/69 (14/69) integration members have zonal wind indexes that are smaller (larger) than a standard deviation of −0.8 (0.8). Figures 1c and d show the composite spatial distribution of 850-hPa horizontal wind anomalies for these negative and positive integration members. The wind anomalies for negative integration members (Fig. 1c) show a tripolar pattern of anomalous centers, resembling well the observed wind anomalies (Fig. 1a). It indicates that the negative index integration members can capture the EAP pattern over the WNP-EA. In contrast, the anticyclonic anomaly over the subtropical WNP in positive integration members (Fig. 1d) extends northward to the midlatitudes, associated with a cyclonic anomalous center to the north of 50°N, which is opposite to that in negative index integrations and observations in the midlatitude regions. The opposite anomalous circulation patterns between negative and positive integration members therefore lead to the weak circulation anomalies in midlatitude regions for MME mean prediction (Fig. 1b), suggesting that large spread exists among model integration members and that the extratropical part of the EAP pattern is reproduced but may not be predictable.

A scatterplot of zonal wind indexes from the 69 integration members in 1998 is shown in Fig. 2 (y-axis). It can be seen that zonal wind indexes are quite dispersed, with about half of the indexes being negative and the other half positive. The zonal wind index in the MME mean prediction is small (0.003 m s^{-1}), while the zonal wind index in observations is −1.40 m s^{-1}. The spread of the ensemble members does include the observed value. In comparison, the subtropical component of the EAP pattern in 1998, represented by the WNP monsoon index (WNPMI) following Wang and Fan (1999) [the 850-hPa zonal wind anomalies between (5°–15°N, 100°–130°E) and (20°–30°N, 110°–140°E)], is well predicted by the ensemble members, as shown in Fig. 2

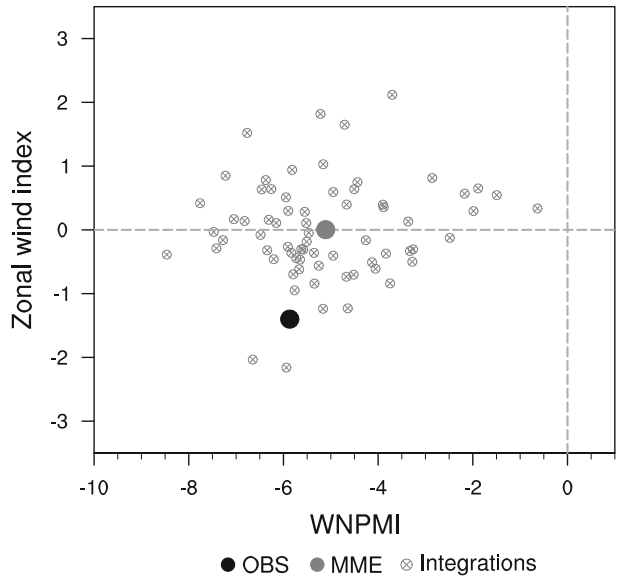

Fig. 2. Scatterplot for the anomalies of the midlatitude zonal wind index (*y*-axis, as shown by the green box in Fig. 1) and WNPMI (*x*-axis) from 69 integrations in 1998. Black and grey dots represent the indexes in the MME mean and observations, respectively. Units: m s^{-1}.

(*x*-axis). Almost all members are negative, indicating that the models are able to simulate and predict the anomalous anticyclonic circulation over the subtropical WNP in 1998. The WNPMI is negative both in the observations and MME mean prediction, and the intensity of circulation anomalies in the MME mean prediction (−5.10 m s^{-1}) is close to that in observations (−5.87 m s^{-1}). This is in accordance with the high prediction skill of the anticyclonic circulation anomaly in the subtropical WNP (Kosaka et al., 2012; Li et al., 2012), which to a large extent contributes to the prediction skill of the EAP index shown previously. However, the correlation coefficient of these ensemble members between the zonal wind index and WNPMI is quite low (0.12), implying a largely independent variation of these two components of the EAP pattern in model predictions in 1998, regardless of strong tropical forcing.

Further evidence of a lack of predictability in the midlatitude component of the EAP pattern can be found from hindcast years besides 1998. The correlation coefficient between the predicted and observed zonal wind indices is only 0.21 (0.23) for all hindcast years of ENSEMBLES (GloSea5). Similarly, the interannual variance of the ensemble mean prediction in ENSEMBLES (GloSea5) is 0.01 (0.03) m^2 s^{-2}, which is much lower than that in observations (0.56 m^2 s^{-2} for 1960–2005 and 0.43 m^2 s^{-2} for 1992–2011), while in all ensemble members, concatenated after subtracting the climatology of individual models from 1992 to 2005, it is 0.42 m^2 s^{-2}, which is similar to that in observation. These results confirm that little prediction skill exists in the midlatitude circulations of the EAP pattern, even though the pattern is realistically simulated by the model. However, there is also some evidence for model error in the teleconnection between the midlatitude zonal wind and the WNP subtropical high: the correlation coefficient between the zonal wind index and the WNPMI in all ensemble members from all hindcast years (1992 to 2005) is 0.07, which is lower than that in observations (0.52 for 1979–2015), but still exceeds the 95% confidence level according to the Student's *t*-test because of the large sample size. This implies that while the models can reproduce an EAP pattern through internal variability, they are not able to reproduce well the tropical–mid-latitude teleconnection, and an improvement in prediction skill may be expected if a better teleconnection to the variation in midlatitude circulation associated with the EAP pattern can be reproduced.

Similar situations exist in the five individual models of ENSEMBLES, and all models show significant inter-member variability (uncertainty of the prediction) for the midaltitude circulation related to the variations in the WNP subtropical high (Li et al., 2012, Fig. 11). In addition, none of these models shows good prediction skill of the zonal wind index; correlations range between −0.11 and 0.21. Differences in model performance might lie in the different parameterizations or residual internal variability among different models and are not discussed further in this study.

3.2. *Response of surface temperature in eastern Russia*

Consistent with the atmospheric circulation, the surface temperature anomalies also show a meridional wave-like pattern with negative anomalies along the mei-yu rainband and positive anomalies over eastern Russia and the subtropical WNP (Fig. 3a). The positive surface temperature anomalies averaged over the land area of eastern Russia (50°–70°N, 120°–160°E) reach 1.16°C. For the MME prediction, the anomalies are quite weak and even have the opposite sign in the midlatitude regions. The averaged temperature anomaly in eastern Russia is only −0.33°C, suggesting a poor prediction of the observed temperature variation.

Furthermore, the surface temperature anomalies over the midlatitude WNP-EA also demonstrate large contrast among different groups of ensemble members, as shown in Fig. 3. For negative index cases (Fig. 3c), the surface temperature anomalies show a relatively similar meridional wave-like pattern to observations (Fig 3a). In contrast, for positive integration members (Fig. 3d), the surface temperature anomalies to the north of 30°N are opposite to those for negative integration members and observations, with negative anomalies in eastern Russia and positive anomalies along 40°N of the WNP-EA. The surface temperature anomalies around the Philippine Sea are positive for both integration groups, corresponding to a good capability of models in predicting tropical temperatures. In general, the integration members that reproduce easterly (westerly) anomalies over the midlatitude regions, tend to predict the EAP teleconnection pattern well (badly), and predict positive (negative) surface temperature anomalies in eastern Russia and negative (positive) anomalies along the mei-yu rainband. Large spread in surface temperature among the integrations is found over the midlatitude regions.

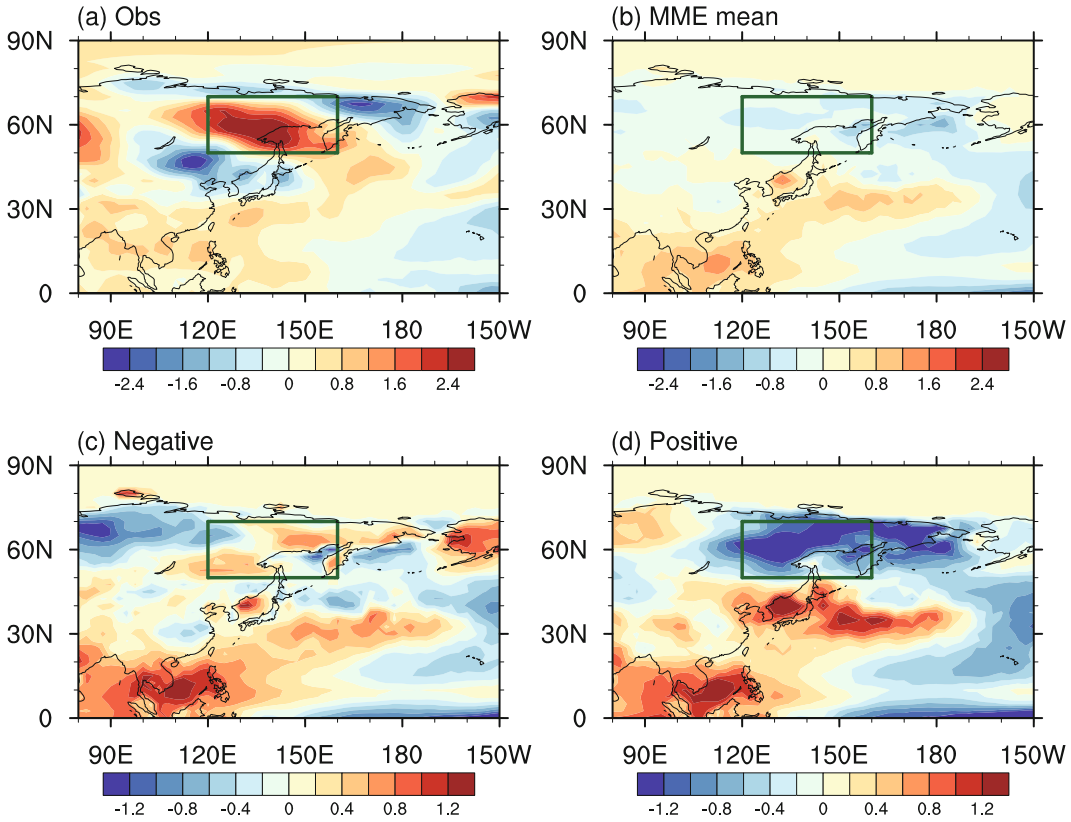

Fig. 3. As Fig. 1 but for surface temperature anomalies (units: °C). The green box indicates the domain of eastern Russia (50°–70°N, 120°–160°E).

An intimate relationship between the midlatitude circulation and surface temperature is further revealed via a scatterplot of surface temperature in eastern Russia and zonal wind index among all model integrations (Fig. 4a). Here, the surface temperature in eastern Russia is defined by the temperature anomalies averaged over the land area in the region (50°–70°N, 120°–160°E). This temperature index and the zonal wind index exhibit a negative relationship, with a correlation coefficient of −0.54, which exceeds the 99% confidence level according to the Student's *t*-test. A positive (negative) surface temperature anomaly in eastern Russia corresponds to an easterly (westerly) anomaly in the midlatitude WNP. Furthermore, the 850-hPa wind anomalies regressed onto the temperature index (Fig. 4b) mainly appear over the midlatitude regions north of 30°N, with an anomalous anticyclone in eastern Russia and a relatively weaker cyclonic anomaly over the WNP-EA. The wind anomalies in the tropics are weak, suggesting that the surface temperatures in eastern Russia are roughly independent of the tropical anomalies in the model integrations.

The relationship between the midlatitude zonal wind anomalies and surface temperature anomalies in eastern Russia not only exists among models integrations, but also in observations, as shown in Fig. 5. The correlation coefficient between the temperature index and zonal wind index for observations during 1979–2015 (Fig. 5a) is −0.60, also exceeding the 99% confidence level according to the Student's *t*-test. This is close to that in the model integrations, suggesting a realistic relationship in the model. Moreover, the 850-hPa wind anomalies related to the surface temperature in eastern Russia (Fig. 5b) resemble well those for models integrations in the extratropical regions (Fig. 4b). In the tropical/subtropical WNP, on the other hand, there is an anticyclonic anomaly in observations, which is absent in model integrations. This difference between the observations and integrations is consistent with the idea that the extratropical part of the EAP is relatively independent of the tropical part in model predictions at least. Given the close relationship between surface temperature in eastern Russia and midlatitude circulation, the limitation of prediction for the extratropical component of the EAP potentially leads to the poor prediction of surface temperature in eastern Russia, and the surface temperature in this region in turn may enhance the spread of midlatitude zonal winds through modulating the meridional gradient of temperatures.

3.3. *Influence on the prediction of East Asian summer rainfall*

Interannual variation of East Asian summer rainfall is significantly affected by the circulation anomalies associated with the EAP teleconnection pattern, particularly the subtropical components (Lu and Dong, 2001; Zhou and Yu, 2005; Yang et al., 2010; Kosaka et al., 2012; Li et al., 2012). This

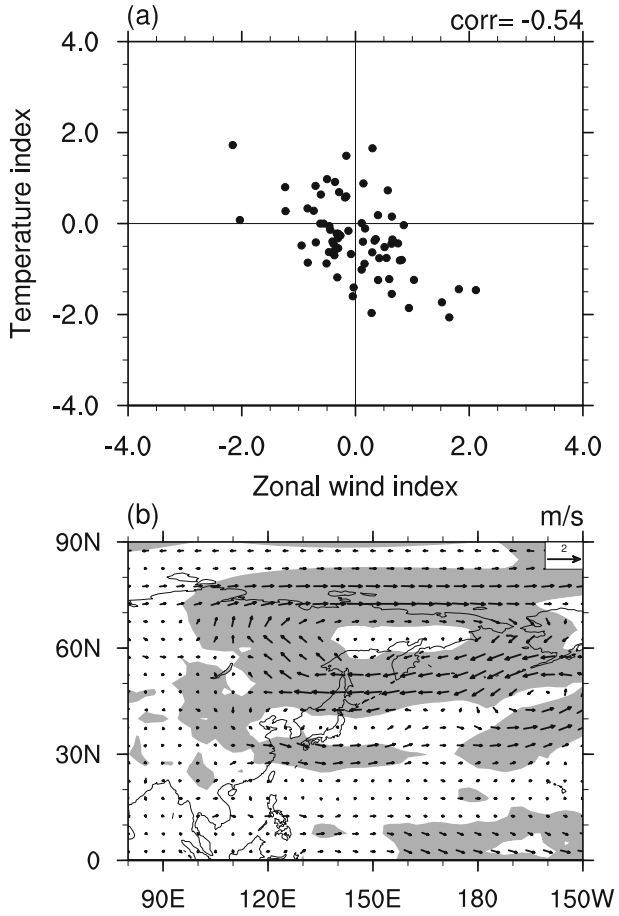

Fig. 4. (a) Scatterplot for the anomalies of temperature index (*y*-axis) and zonal wind index (*x*-axis) from 69 integrations. The temperature index is defined by surface temperature anomalies averaged over the land area in the region (50°–70°N, 120°–160°E), as shown by the green box in Fig. 3. The value in the top-right corner of the diagram is the correlation coefficient between them. (b) 850-hPa horizontal wind anomalies regressed onto the temperature index. Shading indicates regions exceeding the 95% significance level. Units: m s^{-1}.

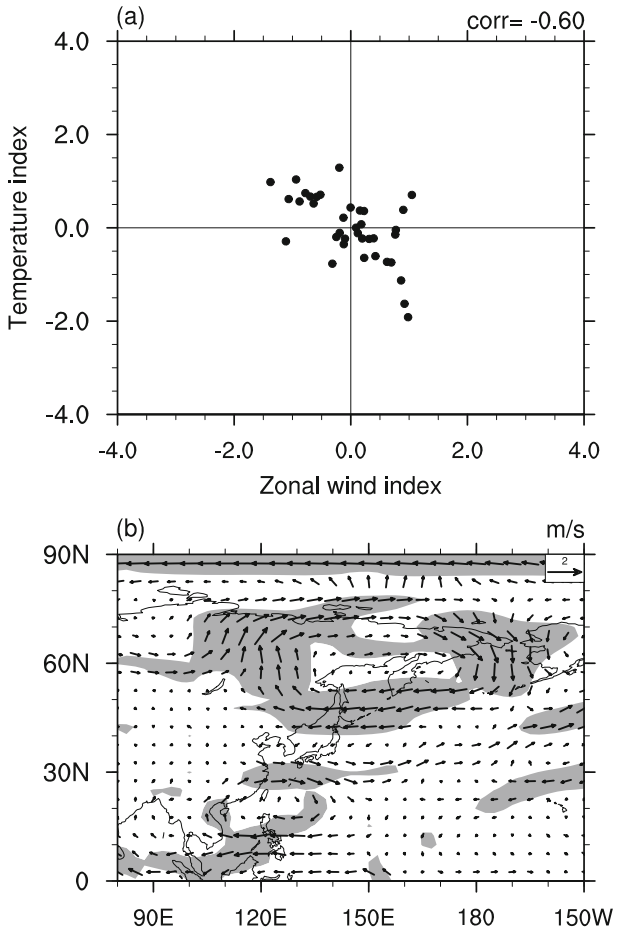

Fig. 5. As in Fig. 4 but for the observations from 1979 to 2015.

section further explores the contribution from midlatitude circulation anomalies described in the preceding section to the East Asian summer rainfall.

Figure 6 shows the distribution of precipitation anomalies in 1998. Corresponding to the atmospheric circulation (Fig. 1), the precipitation also demonstrates a meridional wavelike pattern in observations (Fig. 6a), with positive anomalies along the East Asian mei-yu rainband and negative anomalies around the South China Sea, Philippine Sea and south of eastern Russia. The negative anomalies around the South China Sea and Philippine Sea result in an intensified WNP subtropical high (Fig. 1a), which would further transfer more water vapor to East Asia and induce more rainfall along the East Asian mei-yu rainband. In addition, because of excessive water vapor transported by the midlatitude easterly wind (Fig. 1a), more rainfall also appears around Northeast China, which resulted in serious flooding in the Songhuajiang and Nenjiang basin in that year (Li et al., 2014b).

As the models generally predict the WNP subtropical high (Figs. 1 and 2), they predict well the associated rainfall in the subtropical WNP-EA regions, for both the MME mean and the ensemble members (Figs. 6b–d). However, the MME mean result produces quite weak precipitation anomalies in the midlatitude WNP-EA, including the negative anomalies around the south of eastern Russia and positive anomalies around Northeast China (Fig. 6b). Furthermore, although the models generally reproduce the positive rainfall anomalies along the East Asian mei-yu rainband, the large rainfall over the upper reaches of the Yangtze River basin, Korean Peninsula and the Sea of Japan are also quite weak. The inability of the MME predictions in predicting the above precipitation anomalies connects closely to the lack of skill for the extratropical part of the EAP (Figs. 6c and d). The precipitation anomalies in the negative integrations resemble well those in observations, especially in the midlatitude regions. The positive rainfall anomalies around the upper reaches of the Yangtze River basin, Korean Peninsula and the Sea of Japan are also successfully predicted in these integrations (Fig. 6c). In contrast, in the positive integrations with westerly anomalies in the midlatitude regions, these positive precipitation anomalies together with the midlatitude anomalies do not ap-

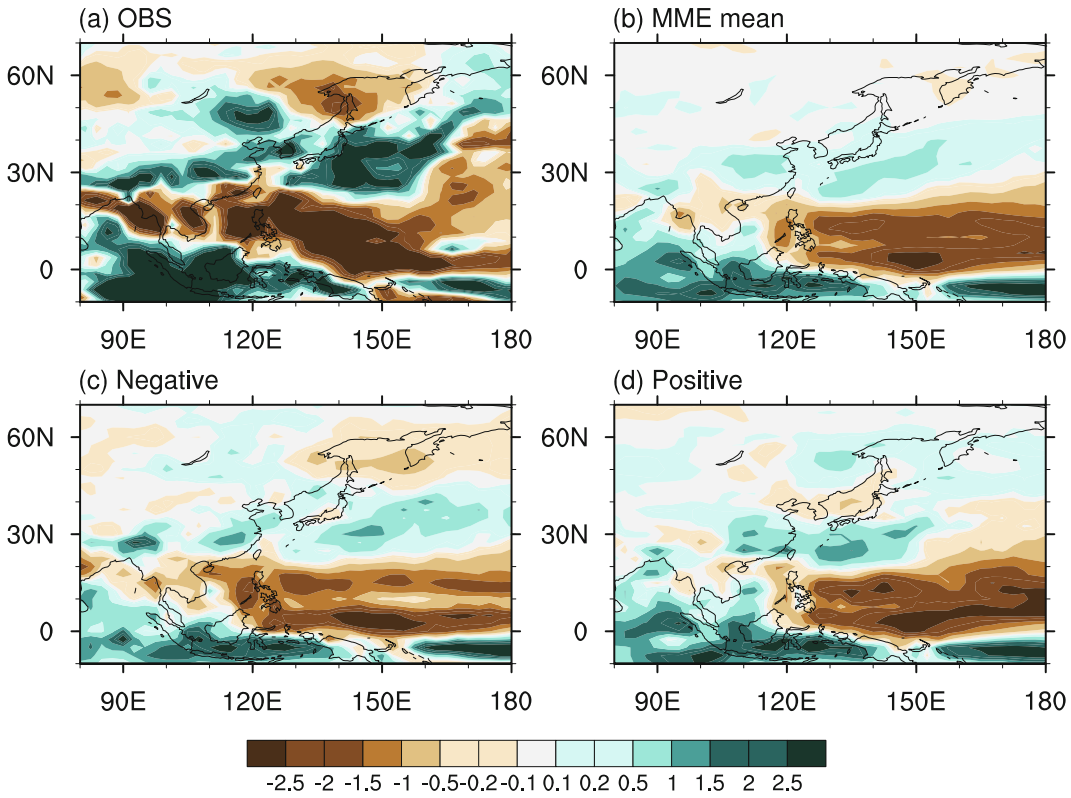

Fig. 6. As in Fig. 3 but for the precipitation anomalies (units: mm d^{-1}).

pear (Fig. 6d), but show an opposite response to the observations and the negative integrations.

The difference between different categories of integrations demonstrate the impact from the midlatitude circulation (Fig. 7). Corresponding to an easterly (westerly) anomaly, less (more) rainfall appears around the south of eastern Russia and more (less) rainfall appears along the East Asian mei-yu rainband. These intimate relationships are detected not just in model integrations from 1998, but also in all ensemble members concatenated after subtracting the climatology of individual models from all overlapping hindcast years and observations for all years from 1979 to 2015. While the precipitation anomalies in 1998 are largely modulated by the WNP subtropical high with strong tropical forcing, these significant relationships further suggest that larger differences in precipitation among integrations could still be anticipated along the East Asian mei-yu rainband, in other years with weak tropical forcing. In summary, the lack of skill in predicting the midlatitude components of the EAP teleconnection pattern suggests a considerable limitation in the seasonal prediction of East Asian summer rainfall, albeit with some potential improvement if modeled tropical teleconnections could be improved.

4. Conclusion

This study focuses on the variation of midlatitude circulation associated with the EAP teleconnection pattern, based on seasonal forecasts from state-of-the-art coupled forecast systems. In association with strong tropical forcing, the EAP teleconnection pattern in 1998, which is typically organized over the WNP-EA in observations, is not well predicted and instead shows quite weak anomalies in the extratropics. The predictions among different model integrations are further investigated to reveal the decoupled tropical–extratropical predictable patterns in models.

A close relationship is detected between the variation of surface temperatures in eastern Russia and midlatitude circulation associated with the EAP pattern, not just among different model integrations, but also among all years in observations. The integrations that predict positive (negative) surface temperature anomalies in eastern Russia tend to reproduce easterly (westerly) anomalies over the midlatitude regions. Similarly, anomalous easterly (westerly) winds tend to appear over the midlatitude WNP/EA in the summer when the surface temperature is warm (cold) in eastern Russia. This coupled relationship increases the uncertainty and difficulty of the prediction of the extratropical component of the EAP pattern and the surface temperature in eastern Russia.

Despite this, the midlatitude circulation anomalies associated with the EAP pattern do significantly modulate East Asian summer rainfall. The integrations predicted with easterly (westerly) anomalies in the midlatitude WNP-EA tend to predict more (less) rainfall along the East Asian mei-yu rainband. As a result, the lack of skill for northern parts of the EAP suggest an important limit to seasonal prediction of

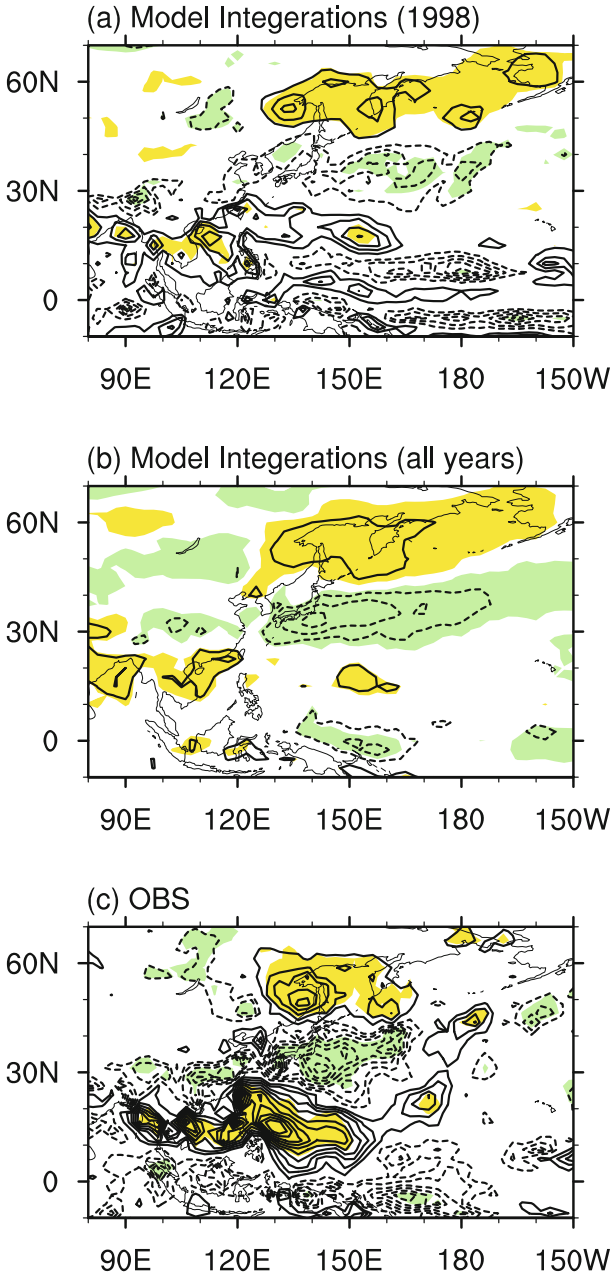

Fig. 7. Precipitation anomalies regressed onto the zonal wind index for model integrations (a) in 1998, (b) from all hindcast years (1992 to 2005) with all ensemble members concatenated after subtracting the climatology of individual models, and (c) in observations for all years from 1979 to 2015. The contour interval is 0.2 mm d^{-1} and shading indicates regions exceeding the 95% significance level.

East Asian summer rainfall, which may be irreducible unless improved teleconnections to the tropics can be simulated in future forecast systems.

Acknowledgements. This study was supported by the National Natural Science Foundation of China (Grant Nos. 41320104007, 41775083 and U1502233). This work and its contributors were also supported by the UK–China Research & Innovation Partnership Fund through the Met Office Climate Science for Service Partnership (CSSP) China as part of the Newton Fund.

REFERENCES

Adler, R. F., and Coauthors, 2003: The version-2 global precipitation climatology project (GPCP) monthly precipitation analysis (1979 Present). *Journal of Hydrometeorology*, **4**, 1147–1167, https://doi.org/10.1175/1525-7541(2003)004<1147:TVGPCP>2.0.CO;2.

Huang, G., 2004: An index measuring the interannual variation of the East Asian summer monsoon—The EAP index. *Adv. Atmos. Sci.*, **21**, 41–52, https://doi.org/10.1007/BF02915679.

Huang, R. H., and F. Y. Sun, 1992: Impacts of the tropical western Pacific on the East Asian summer monsoon. *J. Meteor. Soc. Japan*, **70**, 243–256, https://doi.org/10.2151/jmsj1965.70.1B_243.

Kalnay, E., and Coauthors, 1996: The NCEP/NCAR 40-year reanalysis project. *Bull. Amer. Meteor. Soc.*, **77**, 437–472, https://doi.org/10.1175/1520-0477(1996)077<0437:TNYRP>2.0.CO;2.

Kawamura, R., T. Murakami, and B. Wang, 1996: Tropical and mid-latitude 45-day perturbations over the western Pacific during the northern summer. *J. Meteor. Soc. Japan*, **74**, 867–890, https://doi.org/10.2151/jmsj1965.74.6_867.

Kosaka, Y., and H. Nakamura, 2006: Structure and dynamics of the summertime Pacific-Japan teleconnection pattern. *Quart. J. Roy. Meteor. Soc.*, **132**, 2009–2030, https://doi.org/10.1256/qj.05.204.

Kosaka, Y., S.-P. Xie, N.-C. Lau, and G. A. Vecchi, 2013: Origin of seasonal predictability for summer climate over the Northwestern Pacific. *Proceedings of the National Academy of Sciences of the United States of America*, **110**, 7574–7579, https://doi.org/10.1073/pnas.1215582110.

Kosaka, Y., J. S. Chowdary, S.-P. Xie, Y.-M. Min, and J.-Y. Lee, 2012: Limitations of seasonal predictability for summer climate over East Asia and the Northwestern Pacific. *J. Climate*, **25**, 7574–7589, https://doi.org/10.1175/JCLI-D-12-00009.1.

Li, C. F., R. Y. Lu, and B. W. Dong, 2012: Predictability of the western North Pacific summer climate demonstrated by the coupled models of ENSEMBLES. *Climate Dyn.*, **39**, 329–346, https://doi.org/10.1007/s00382-011-1274-z.

Li, C. F., R. Y. Lu, and B. W. Dong, 2014a: Predictability of the western North Pacific summer climate associated with different ENSO phases by ENSEMBLES multi-model seasonal forecasts. *Climate Dyn.*, **43**, 1829–1845, https://doi.org/10.1007/s00382-013-2010-7.

Li, C., and Coauthors, 2016: Skillful seasonal prediction of Yangtze River valley summer rainfall. *Environmental Research Letters*, **11**, 094002, https://doi.org/10.1088/1748-9326/11/9/094002.

Li, C. F., W. Chen, X. W. Hong, and R. Y. Lu, 2017: Why was the strengthening of rainfall in summer over the Yangtze River valley in 2016 less pronounced than that in 1998 under similar preceding El Niño events?—Role of midlatitude circulation in August. *Adv. Atmos. Sci.*, **34**(11), 1290–1300, https://doi.org/10.1007/s00376-017-7003-8.

Li, Y. S., Y. Q. Xu, and Y. Wang, 2014b: Comparative analysis on flood cause in the Nenjiang basin between 2013 and 1998. *Meteorological and Environmental Research*, **5**, 16–21, 25.

Lu, R. Y., 2001: Atmospheric circulations and sea surface temper-

atures related to the convection over the western Pacific warm pool on the interannual scale. *Adv. Atmos. Sci.*, **18**, 270–282, https://doi.org/10.1007/s00376-001-0019-z.

Lu, R. Y., 2004: Associations among the components of the East Asian summer monsoon system in the meridional direction. *J. Meteor. Soc. Japan*, **82**, 155–165, https://doi.org/10.2151/jmsj.82.155.

Lu, R. Y., and B. W. Dong, 2001: Westward extension of North Pacific subtropical high in summer. *J. Meteor. Soc. Japan*, **79**, 1229–1241, https://doi.org/10.2151/jmsj.79.1229.

Lu, R. Y., and Z. D. Lin, 2009: Role of subtropical precipitation anomalies in maintaining the summertime meridional teleconnection over the Western North Pacific and East Asia. *J. Climate*, **22**, 2058–2072, https://doi.org/10.1175/2008JCLI2444.1.

MacLachlan, C., and Coauthors, 2015: Global Seasonal forecast system version 5 (GloSea5): a high-resolution seasonal forecast system. *Quart. J. Roy. Meteor. Soc.*, **141**, 1072–1084, https://doi.org/10.1002/qj.2396.

Nitta, T., 1987: Convective activities in the tropical western Pacific and their impact on the northern hemisphere summer circulation. *J. Meteor. Soc. Japan*, **65**, 373–390, https://doi.org/10.2151/jmsj1965.65.3_373.

Scaife, A. A., and Coauthors, 2017: Tropical rainfall, Rossby waves and regional winter climate predictions. *Quart. J. Roy. Meteor. Soc.*, **143**, 1–11, https://doi.org/10.1002/qj.2910.

Van Der Linden, P., and J. F. B. Mitchell, 2009: ENSEMBLES: climate change and its impacts: summary of research and results from the ENSEMBLES project. GOCE-CT-2003-505539, Met Office Hadley Centre, FitzRoy Road, Exeter EX1 3PB, UK, 160 pp.

Wang, B., and Z. Fan, 1999: Choice of South Asian summer monsoon indices. *Bull. Amer. Meteor. Soc.*, **80**, 629–638, https://doi.org/10.1175/1520-0477(1999)080<0629:COSASM>2.0.CO;2.

Wang, B., and Coauthors, 2009: Advance and prospectus of seasonal prediction: assessment of the APCC/CliPAS 14-model ensemble retrospective seasonal prediction (1980-2004). *Climate Dyn.*, **33**, 93–117, https://doi.org/10.1007/s00382-008-0460-0.

Wang, B., R. G. Wu, and X. H. Fu, 2000: Pacific-East Asian teleconnection: How does ENSO affect East Asian climate? *J. Climate*, **13**, 1517–1536, https://doi.org/10.1175/1520-0442(2000)013<1517:PEATHD>2.0.CO;2.

Xie, S.-P., Y. Kosaka, Y. Du, K. M. Hu, J. S. Chowdary, and G. Huang, 2016: Indo-western Pacific ocean capacitor and coherent climate anomalies in post-ENSO summer: A review. *Adv. Atmos. Sci.,* **33**, 411–432, https://doi.org/10.1007/s00376-015-5192-6.

Yang, R. W., Y. Tao, and J. Cao, 2010: A mechanism for the interannual variation of the early summer East Asia-Pacific teleconnection wave train. *Acta Meteorologica Sinica*, **24**, 452–458.

Zhou, T.-J., and R. C. Yu, 2005: Atmospheric water vapor transport associated with typical anomalous summer rainfall patterns in China. *J. Geophys. Res.*, **110**, D08104, https://doi.org/10.1029/2004JD005413.